ChemPubSoc Europe

DOI: 10.1002/open.201600109

Open Access ChemistryOPEN Communications

Facile Preparation of Chloride-Conducting Membranes: First Step towards a Room-Temperature Solid-State Chloride-Ion Battery

Fabienne Gschwind,*[a] Dominik Steinle,[a] Daniel Sandbeck,[a] Celine Schmidt,[a] and Elizabeth von Hauff[b]

Three types of chloride-conducting membranes based on polyvinyl chloride, commercial gelatin, and polyvinyldifluoride-hexafluoropolymer are introduced in this report. The polymers are mixed with chloride-containing salts, such as tetrabutylammonium chloride, and cast to form membranes. We studied the structural properties, thermal stability, and electrochemical response of the membranes to understand chloride migration and transport. Finally, the membranes are tested in a prototype solid-state chloride-ion battery setup. The feasibility of the membranes for their potential use in anion batteries is discussed.

Chloride-conducting materials are interesting for applications such as sensing purposes,[1–3] biological membrane transport[4–6] and, very recently, for chloride-ion batteries (CIBs).[7–11]

Many high-temperature chloride conductors exist already and substantial progress has been made in recent decades.[12–17] Nevertheless, few chloride conductors based on polymers have been reported, such as plasticized quaternary ammonium polymers[18,19] where poly(diallyldimethylammonium chloride) is used as a fast anion conductor. Hardy and Shriver showed that the ion mobility is only attributed to the chloride and that the use of a plasticizer reduced the tight ion pairing, inducing a beneficial effect on chloride mobility.[18] A series of investigations conducted on chloride transport in cells and tissues[4,20] unveiled that chloride ions are transported through special channels in and out of cells. Furthermore, anion-exchange membranes[21,22] were developed to exchange halogenide species that can also be used as a basis to understand transport mechanisms. Also, ionophores (carrier molecules), which selectively transport chloride ions, are known and have been used for sensing purposes.[1–3,23–25]

[a] Dr. F. Gschwind, D. Steinle, D. Sandbeck, C. Schmidt
Helmholtz Institute Ulm for Electrochemical Energy Storage (HIU)
Helmholtzstrasse 11, 89081 Ulm (Germany)
E-mail: fabienne.gschwind@kit.edu

[b] Prof. Dr. E. von Hauff
Department of Physics and Astronomy, VU Amsterdam
De Boelelaan 1081, 1081 HV Amsterdam (The Netherlands)

Supporting Information for this article can be found under http://dx.doi.org/10.1002/open.201600109.

Conducting membranes (or *gel electrolytes*) are widely applied in lithium-ion battery technologies.[24–26] In general, the prerequisites of a good gel electrolyte can also be applied to a chloride-conducting membrane: 1) high ionic conductivity, 2) stable in air, 3) mechanical strength, 4) good transference number, 5) thermal and electrochemical stability, and 6) compatibility with electrodes.

Until now, only ionic liquids (ILs), such as 1-methy-3-octylimidazolim chloride mixed with 1-butyl-3-methylimidazolium chloride or 1-butyl-1-methylpiperidinium bis-(trifluoromethylsulfonyl)imide in propylene carbonate,[7–11] have been used in CIBs. The main problem of CIBs with ILs is dissolution of the anode and cathode materials.

Owing to dissolution of the cathode material, only a few cycles can be obtained in batteries with simple chloride salts such as $CuCl_2$ or $BiCl_3$.[7] Furthermore, dissolution of the electrode materials can lead to unexpected side reactions when lithium or magnesium cations travel through the electrolyte, resulting in erroneous capacity or battery performance. Efforts have been made to identify stable cathode materials, with several publications focusing on the use of air-sensitive oxychlorides in CIBs.[9–11]

The advantage of CIBs is that chloride sources are sustainable and widely available, making it interesting for large-scale and cheap storage applications, especially if the materials are air stable and can be handled without the need for special equipment. This would compensate for the lower energy density disadvantage of CIBs.

We investigated air-stable gel membranes, which can be applied as cathodes in combination with common chloride salts ($CuCl_2$, $BiCl_3$), or even in combination with organic cathodes such as polyaniline (PANI).[27,28] Such membrane-based dry battery systems have many advantages, such as no leakage, because no volatile or flammable solvents are required. Furthermore, the dissolution of the electrode is avoidable. Finally, polymer-membrane-based CIBs have potential in a flexible design using printing technologies, similar to widely studied all-polymer batteries, which are mostly based on organic redox-active polymers.[29–32]

In this work, we synthesized and characterized chloride-conducting membranes for application in CIBs. A working principle for the oxidation of the anode and reduction of the cathode is shown in Figure 1.

We selected three simple polymer-electrolyte systems that are widely known in lithium or sodium battey systems. Namely, polyvinylchloride (PVC) and polyvinyldifluoride-hexafluoropolymer (PVDF-HF) as well as commercial gelatin were evaluated

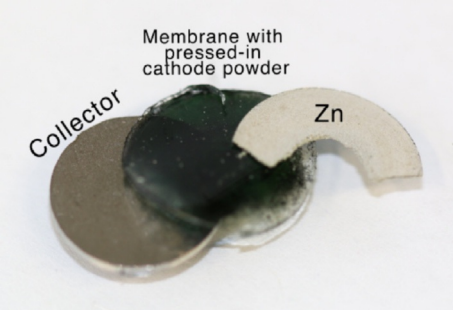

Figure 1. Working principle and cell configuration of CIBs utilizing chloride-conducting membranes.

when combined with chloride salts containing large cations, such as tetraethyl ammonium chloride (for gelatin), tetrabutyl ammonium chloride (TBACl) for the PVDF-HF membrane, and octyltrimethyl ammonium chloride (TOACl) for the PVC membrane.

The different membranes were prepared according to the process explained in the Experimental Section (in the Supporting Information). Gelatin membranes were made by soaking commercial gelatin powder in dimethylsulfoxide (DMSO) and subsequently reacting it with tetraethylammonium chloride (TEACl) (Figure 2a). PVC membranes were made by combining PVC and TOACl with phthalate plasticizer (Figures 2b and 2c). The PVDF-HF membrane was prepared by mixing PVDF-HF with PEG400 as the plasticizer and TBACl. The resulting film resembled fluffy cotton wool rather than a polymer electrolyte (Figure 2c).

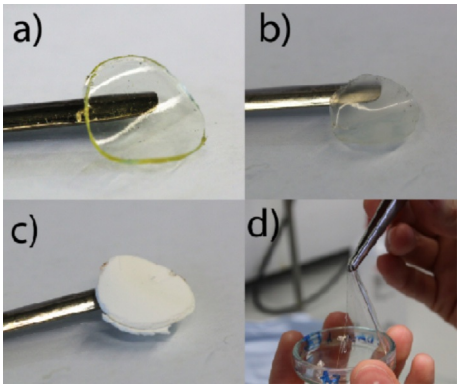

Figure 2. Digital photographs of the three freestanding membranes: a) gelatin, b) PVC, c) PVDF-HF, and d) PVC stability evaluation.

IR analysis of the membranes confirmed that the matrix contains the starting materials, whereas the XRD patterns confirmed that the crystalline chloride salts have been embedded in the polymer (Supporting Information).

The thermal stability of the three samples was assessed to evaluate their suitability for practical battery applications. PVC showed thermal stability for temperatures up to 150 °C, followed by a rapid weight loss. This is probably caused by a release of the tetrahydrofuran (THF) solvent together with the

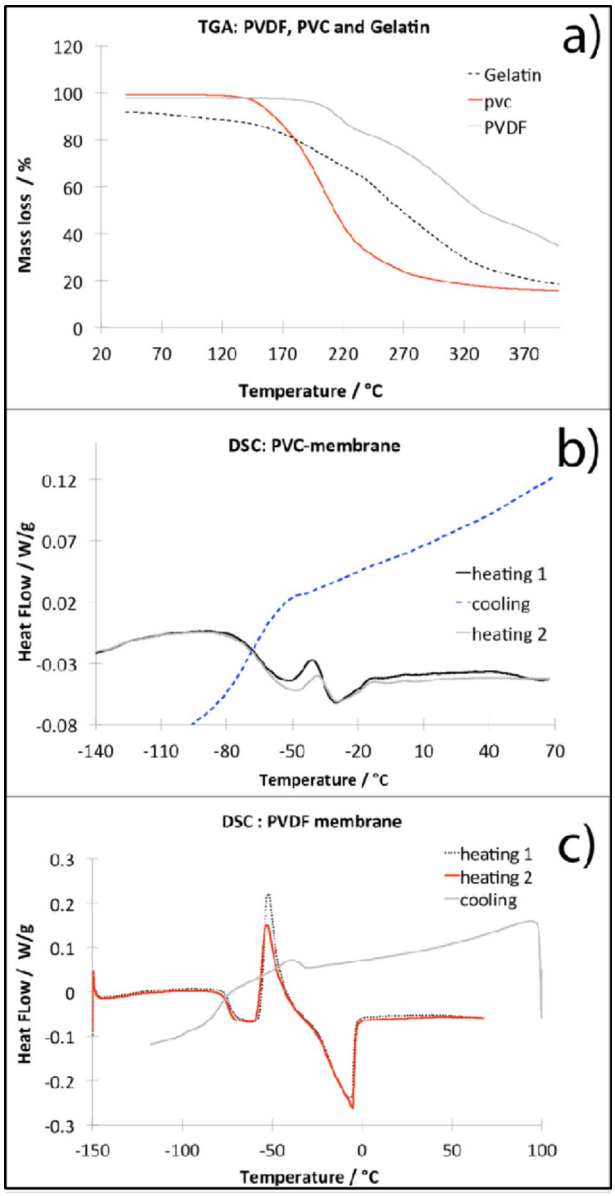

Figure 3. a) TGA of all three membranes, b) DSC of PVDF, and c) DSC of PVC.

decomposition of the membrane matrix starting from approximately 150 °C (Figure 3a). As expected, the gelatin membrane shows a strong release of solvent, whereas its thermal decomposition seems to commence at 200 °C. PVDF-HF appears to be stable up to 220 °C before it slowly decomposes. Differential scanning calorimetry (DSC) was performed on the PVC and PVDF-HF membranes, respectively. The gelatin membrane was excluded, owing to its strong DMSO release at low temperatures. For PVDF-HF, the heating curves show a cold crystallization at between −70 and −60 °C immediately after smelting at about −60 °C. Furthermore, a second smelting can be observed between −40 and −5 °C. The first cold crystallization is new and cannot be attributed to the PVDF-HF matrix and might be caused by the chloride salt. The second transitions can be attributed to the glass transition of PEG400 (Figure 3b and the Supporting Information). During the initial heating,

PVC shows an uncommon positive heat-flow change, which might be caused by chain movement of the polymer. At −45 °C, a double glass transition can be observed, possibly owing to the PVC matrix and phthalate plasticizer. The peaks are fairly broad, indicating a large chain distribution of PVC. At 55 °C, a mass change occurs, possibly owing to the evaporation of THF, which subsequently shifts the second heating curve (Figure 3 c).

Further tests were performed by using electrochemical impedance spectroscopy (EIS) and cyclic voltammetry (CV).

CV studies do not show any special features and the electrochemical window for PVDF-HF and PVC lies between −2 and 2 V, whereas gelatin has a stability window between −2.2 and 2.2 V. As seen in Figure 4, for PVDF-HF and PVC, no artefacts can be observed, whereas gelatin displays a broad peak at around −1 V and also at around 2 V. The CV was repeated under different test conditions (different electrodes, different membrane thickness, different composition), but the feature was always visible. Owing to the large amount of solvent, we assume that the feature may originate from dissolved oxygen or water in the DMSO solvent, which could be responsible for oxidation and reduction reactions.

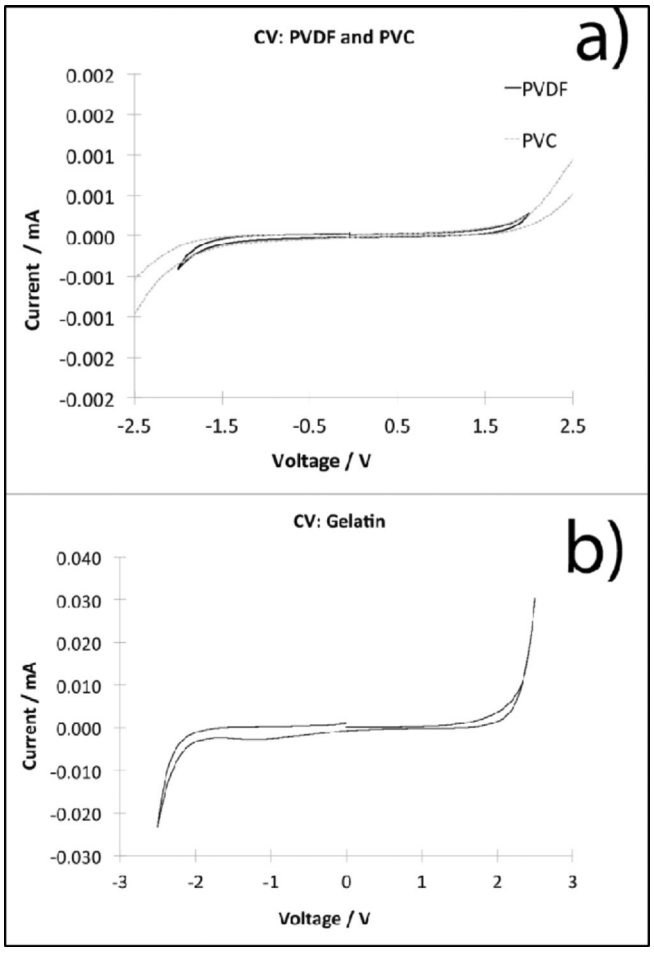

Figure 4. CV of a) PVDF and PVC and b) gelatin, measured from −2.5 to 2.5 V at a scan rate of 20 mV s^{-1}.

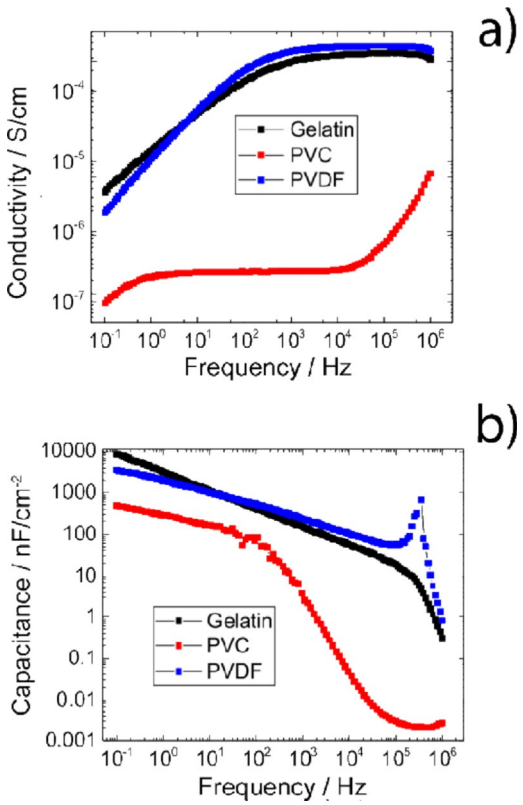

Figure 5. EIS spectra of all three electrodes. a) The Cole–Cole plot of the impedance data; the imaginary component of Z (Im Z) is plotted against the real component (Re Z). b) The conductivity versus frequency of the three membranes.

All of the membranes demonstrate a decrease in conductivity at low frequencies (Figure 5 a), which is consistent with electrode polarization through the formation of an ionic double layer. At intermediate frequencies, the conductivity plateaus and the DC conductivity can be determined in this regime. The conductivity of the PVC membrane is very low (10^{-7} S cm^{-1} at 25 °C) and, therefore, poor battery performance can be expected. For gelatin and PVDF-HF, the conductivity is three orders of magnitude higher (10^{-4} S cm^{-1} at 25 °C). At higher frequencies, the conductivity of the PVC membrane increases, which is consistent with dispersive ionic transport.[35] We attribute the lower conductivity in PVC to both a lower concentration as well as lower mobility of ions in this membrane. The capacitance versus frequency is plotted in Figure 5 b. Gelatin and PVDF-HF demonstrate very similar capacitance values over the entire frequency range. At low frequencies, the capacitance is nearly 10 000 nF cm^2 and decreases with increasing frequency. PVC, on the other hand, demonstrates capacitance values that are almost an order of magnitude lower at low frequencies.

We also observe a different frequency-dependent behavior in frequency spectra from PVC. For this sample, capacitance values begin to drop more rapidly with frequency starting at 100 Hz (Supporting Information). This corresponds to a relaxation peak in the Cole–Cole spectra. In contrast, no relaxation peak is observed in the Cole–Cole spectra taken from the gelatin and PVDF-HF membranes, indicating that ionic mobility in

these samples occurs on faster time scales than we observe with impedance spectroscopy.

The cell tests were performed in a two-electrode Swagelok-type battery cell, assembled under ambient conditions. For the cathode material, $CuCl_2 \cdot 4H_2O$ was ball-milled with carbon black (acetylene black) and TBACl in a ratio (wt%) of 70:20:10. A piece of membrane material was punched into a disc (11–12 mm diameter) and 1 mg of cathode material was spread onto the surface and carefully pressed into the membrane disc (Figure 6). On the other side, a piece of Zn was placed and carefully pressed into the membrane.

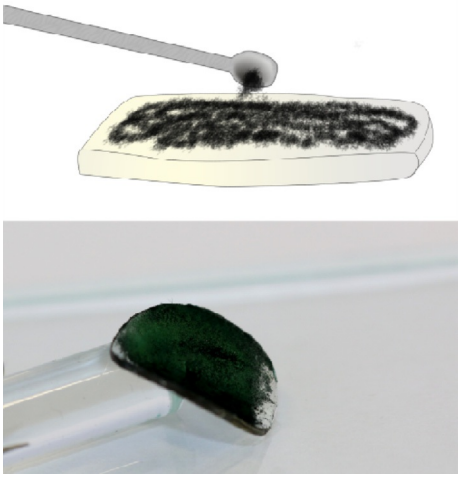

Figure 6. Simple preparation of the electrode; the cathode powder is simply pressed into the surface. Photo: Gelatin membrane prepared with PANI.

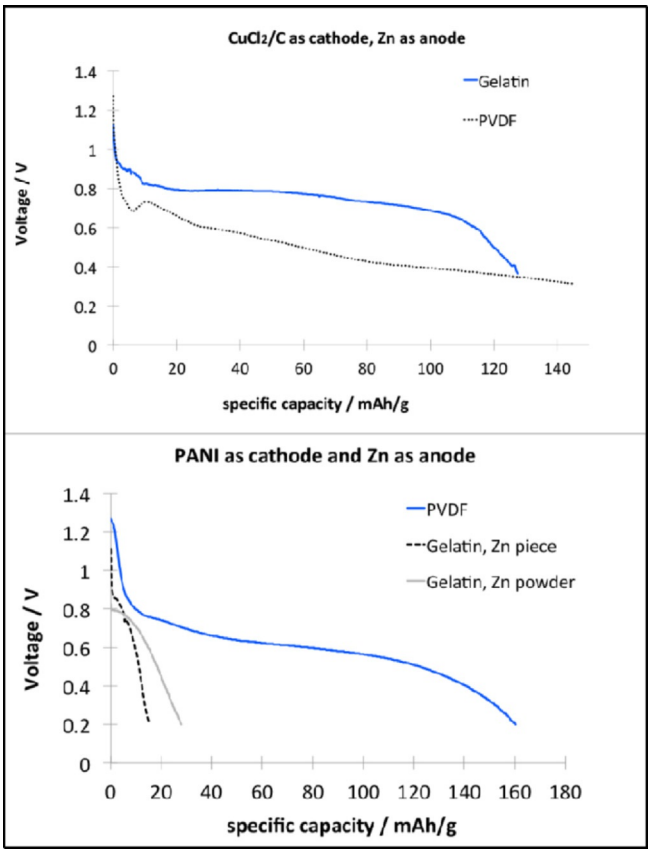

Figure 7. Discharge curves of PVDF and gelatin combined with $CuCl_2$/C and PANI as the cathode material, respectively.

This simple setup allowed us to assess the feasibility of the membranes in CIBs, and we did not focus on cathode optimization. Incorporation of a cathode material into the electrolyte in further studies will allow for a more efficient assessment.

The discharge was performed at room temperature by using a constant current of $7 \cdot 10^{-6}$–$1 \cdot 10^{-5}$ A. Interestingly, the $CuCl_2$ cathode shows the best performance in combination with the gelatin membrane, whereas the PANI cathode operates well when combined with the PVDF-HF membrane. It is not clear from our analysis why PVDF-HF performs best in combination with PANI and gelatin fails completely. For both cathodes, the open-circuit voltage (OCV) started between 1.5 and 1.2 V followed by a drop, possibly owing to poor ionic conductivity of the cathode material or because of poor contact. The discharge plateau occurs between 0.8 and 0.9 V for the $CuCl_2$ cathode and between 0.6 and 0.8 V for PANI. Discharge capacities of around 120 and 150 mAh g^{-1} can be observed (Figure 7). This result is similar to other air-stable all-polymer batteries[29–32,34] and a promising start for our very rudimental battery setup.

As expected, PVC showed only poor electrochemical performance, even at elevated temperature (50 °C) and is not represented here (Supporting Information). $CuCl_2$ was used to assess whether Cu^{2+} ions penetrate or migrate through the membrane. We expect a blue–green coloration of the membrane in the case of a reaction with the cathode. However, we only observed coloration of the membrane at points where it was directly in contact with the $CuCl_2$ powder.

To evaluate the electrochemical and possible side reactions, the anode and cathode were subjected to post-mortem analysis by using scanning electron microscopy combined with energy-dispersive X-ray spectroscopy (SEM/EDX) and XRD. The anode was characterized by using SEM/EDX to detect a $ZnCl_2$ deposit. It is worth noting that this evaluation was difficult, owing to the strong adhesion between the membrane and the current collector, as alterations of the surface as well as contaminations originating from the cathode material are possible (Figure 8c). For all membranes, the formation of deposits on the Zn anode is visible, (Figures 8a and 8b), and only parts of the anode surface are covered with Zn-chloride species (possibly $ZnCl_2$, Zn-oxychloride, or $ZnCl_2$ hydrates). This is likely caused by an uneven contact between the anode, membrane, and current collector.

Although the PVC membrane showed only poor discharge performance, hexagonal particles could still be observed on the Zn anode, indicating that the conversion reaction took place even in this setup (Figure 8a).

Occasionally, "Zn-chloride" crystal depositions are found in the first layer of the membrane, particularly in the case of the PVC membrane (Figure 8d). We suspect that Zn^{2+} diffusion occurs at the contact point between the Zn anode and the

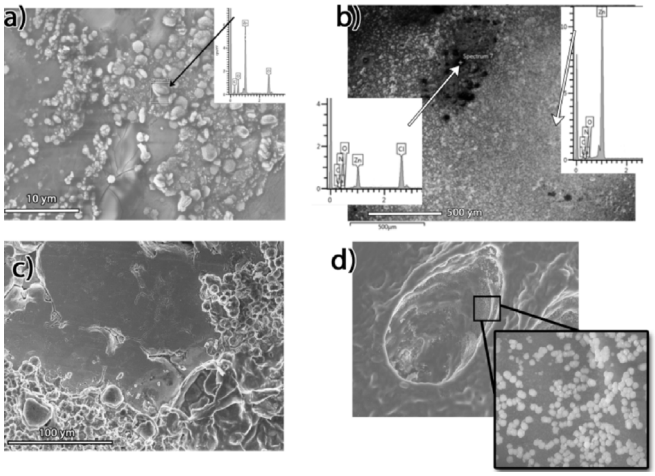

Figure 8. SEM and EDX of the Zn anode after discharge combined with a) the PVC membrane (Zn-chloride crystallites are visible), b) the gelatin membrane (uneven distribution of ZnCl deposits), and c) the PVDF-HF membrane (firmly sticking to the surface of the anode; d) SEM images of Zn-chloride species formation on the membrane (PVC) itself.

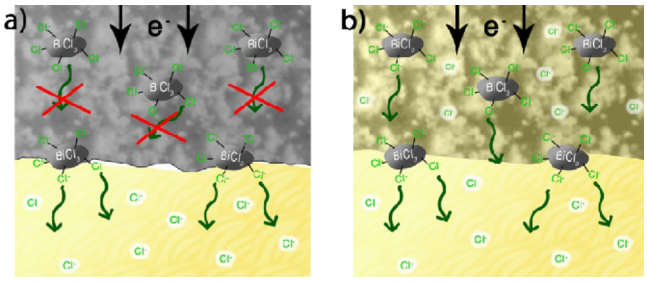

Figure 9. a) The membrane is placed directly on a slurry-coated electrode inducing poor contact, and only the top most level directly in contact with the membrane is involved in electrochemical reactions. b) Polymer composite electrodes would comprise the electrode material directly embedded in the chloride-conducting membrane along with electron conducting species.

membrane, with the subsequent formation of "ZnCl" in cavities at the surface of the membrane (more details in the Supporting Information).

To confirm that the reduction reaction took place, XRD measurements were performed. In a few cases, it was possible to see the formation of metallic copper with the naked eye; however, it remains to be confirmed that this is not an indication for problems inside the battery, such as short circuiting.

Nevertheless, conclusive XRD patterns indicating the existence of "$Cu^{I}Cl$" or even Cu could not be obtained by using $CuCl_2$ pressed onto the membrane and Zn particles present on the other side. We, therefore, switched to $BiCl_3$/BiOCl, as bismuth metal generates a pair of very characteristic peaks and can thus be used to detect changes in anion batteries.[35–37] Afterwards, discharge XRD analysis was performed; the broad diffraction signal of the polymer is visible as well as the characteristic peaks of metallic Bi (Supporting Information).

Based on these observations, we assume that our membrane batteries behave as CIBs. The conductivity in the membranes is rather low compared to the IL mixtures commonly used in chloride-ion batteries. Another limitation in membrane electrolytes is that electrochemical reactions can only occur at the electrode–electrolyte interphase (Figure 9a).

This means that polymer composite electrodes (cathode materials combined with electrolyte and electron-conducting materials) and improved anode systems are required for future developments of this battery system.

Our results show that no "metal migration" through the membrane has taken place; however, as no cycling was performed for the first tests, it is unclear if this will be an issue in future. In that case, the use of complexing agents may prevent migration of metal cations. Furthermore, the transformation of metal salts to pure metals may cause the growth of dendrites through the membrane, causing short circuiting. This could be circumvented with optimized battery design, including the incorporation of separators in the membrane.

In summary, three chloride-conducting polymer membranes were prepared based on the well-known polymer matrices PVC, PVDF-HF, and gelatin combined with commercial chloride salts. Analytical tools were applied to characterize the membranes and full incorporation of the chloride salts was confirmed by using XRD. TGA showed thermal stability up to 150 °C for the PVC membranes. Higher stability was observed for both the PVDF-HF and gelatin membranes. For the gelatin membrane, a heavy loss of solvent upon heating was observed. EIS measurements indicated chloride-ion migration. PVC provided the lowest conductivity (10^{-7} S cm^{-1}), whereas the other membranes demonstrated conductivity values above 10^{-4} S cm^{-1}, which is acceptable for such types of solid electrolytes.

For prototype battery tests, a simple construction method was used. The cathode and anode materials are pressed on each side of the membrane at ambient conditions. $CuCl_2$/C powder was used as the cathode material, PANI salt was applied as the organic cathode, and a piece of Zn was used as the anode. This rudimental setup showed a low OCV of 1.2 V and a discharge plateau at around 0.8 V, with reproducible discharge curves. Low performances can be attributed to poor connections of the different interphases (ionic as well as electric) as well as to the use of low-cost materials. The conversion of Zn to "Zn-chloride" species could be confirmed through SEM/EDX observations, and the conversion of the cathode side was monitored by XRD using the transformation of $BiCl_3$/BiOCl to Bi.

It can be concluded that the use of solid membrane electrolytes appears to be feasible and, thus, could be promising for future applications in CIBs. This system would be particularly promising when the cathode and anode materials are incorporated in the membrane electrolyte and a fully flexible all-polymer battery could be constructed.

Currently, the charging behaviors are being investigated along with deeper studies on chloride migration.

Acknowledgements

The authors would like to thank Marlou Keller and Irene Osada for help with the TGA and DSC analysis. We acknowledge support by Open Access Publishing Fund of Karlsruhe Institute of Technology.

Keywords: anion migration · chloride conductivity · chloride-ion batteries · gel electrolytes · membranes

[1] F. Zapata, A. Caballero, A. Espinosa, A. Tárraga, P. Molina, *J. Org. Chem.* **2008**, *73*, 4034 – 4044.
[2] S. S. S. Tan, P. C. Hauser, K. Wang, K. Fluri, K. Seiler, B. Rusterholz, G. Suter, M. Krüttli, U. E. Spichiger, W. Simon, *Anal. Chim. Acta* **1991**, *255*, 35 – 44.
[3] R. Long, E. Bakker, *Anal. Chim. Acta* **2004**, *511*, 91.
[4] N. P. Illsley, A. S. Verkman, *Biochemistry* **1987**, *26*, 1215 – 1219.
[5] D. G. Warnock, V. J. Yee, *J. Clin. Invest.* **1981**, *67*, 103 – 115.
[6] M. Dalmark, *J. Physiol.* **1975**, *250*, 39 – 64.
[7] X. Zhao, S. Ren, M. Bruns, M. Fichtner, *J. Power Sources* **2014**, *245*, 706 – 711.
[8] X. Zhao, Q. Li, Z. Zhao-Karger, P. Gao, K. Fink, X. Shen, M. Fichtner, *ACS Appl. Mater. Interfaces* **2014**, *6*, 10997 – 11000.
[9] P. Gao, X. Zhao, Z. Zhao-Karger, T. Diemant, R. J. Behm, M. Fichtner, *ACS Appl. Mater. Interfaces* **2014**, *6*, 22430 – 22435.
[10] P. Gao, M. A. Reddy, X. Mu, T. Diemant, L. Zhang, Z. Zhao-Karger, V. S. K. Chakravadhanula, O. Clemens, R. J. Behm, M. Fichtner, *Angew. Chem.* **2016**, *128*, 4357 – 4362.
[11] X. Zhao, Z. Zhao-Karger, D. Wang, M. Fichtner, *Angew. Chem. Int. Ed.* **2013**, *52*, 13621 – 13624; *Angew. Chem.* **2013**, *125*, 13866 – 13869.
[12] N. Imanaka, K. Okamoto, G. Y. Adachi, *Angew. Chem. Int. Ed.* **2002**, *41*, 3890 – 3892; *Angew. Chem.* **2002**, *114*, 4046 – 4048.
[13] N. Imanaka, K. Okamoto, G. Y. Adachi, *Electrochem. Commun.* **2001**, *3*, 49 – 51.
[14] H. Hoshino, M. Yamazaki, Y. Nakamura, M. Shimoji, *J. Phys. Soc. Jpn.* **1969**, *26*, 1422 – 1426.
[15] K. Okamoto, *Solid State Ionics* **2002**, *154 – 155*, 577 – 580.
[16] S. D. Kirik, E. G. Yakovleva, A. F. Shimanskii, Y. G. Kovalev, *Acta Crystallogr. Sect. C* **2001**, *57*, 1367 – 1368.
[17] I. V. Murin, O. V. Glumov, N. A. Mel'nikova, *Russ J Electrochem* **2009**, *45*, 411 – 16.
[18] L. C. Hardy, D. F. Shriver, *Macromolecules* **1984**, *17*, 975 – 977.
[19] J. Qiao, J. Zhang, J. Zhang, *J. Power Sources* **2013**, *237*, 1 – 4.
[20] A. V. Koulov, T. N. Lambert, R. Shukla, M. Jain, J. M. Boon, B. D. Smith, H. Li, D. N. Sheppard, J.-B. Joos, J. P. Clare, A. P. Davis, *Angew. Chem. Int. Ed.* **2003**, *42*, 4931 – 4933; *Angew. Chem.* **2003**, *115*, 5081 – 5083.
[21] G. Merle, M. Wessling, K. Nijmeijer, *J. Membr. Sci.* **2011**, *377*, 1 – 35.
[22] V. K. Shahi, S. K. Thampy, R. Rangarajan, *J. Membr. Sci.* **1999**, *158*, 77 – 83.
[23] K. P. Xiao, P. Bühlmann, S. Nishizawa, S. Amemiya, Y. Umezawa, *Anal. Chem.* **1997**, *69*, 1038 – 1044.
[24] Y.-L. S. Tse, H. N. Sarode, G. E. Lindberg, T. A. Witten, Y. Yang, A. M. Herring, G. A. Voth, *J. Phys. Chem. C* **2014**, *118*, 845 – 853.
[25] J. Y. Song, Y. Y. Wang, C. C. Wang, *J. Power Sources* **1999**, *77*, 183 – 197.
[26] A. Manuel Stephan, *Eur. Polym. J.* **2006**, *42*, 21 – 42.
[27] J. E. Frommer, *Acc. Chem. Res.* **1986**, *19*, 2 – 9.
[28] H. Karami, M. F. Mousavi, M. Shamsipur, *J. Power Sources* **2003**, *117*, 255 – 259.
[29] J. Wang, C. O. Too, G. G. Wallace, *J. Power Sources* **2005**, *150*, 223 – 228.
[30] D. Mecerreyes, R. Marcilla, E. Ochoteco, H. Grande, J. A. Pomposo, R. Vergaz, J. M. Sánchez Pena, *Electrochim. Acta* **2004**, *49*, 3555 – 3559.
[31] I. Sultana, M. M. Rahman, J. Wang, C. Wang, G. G. Wallace, H.-K. Liu, *Electrochim. Acta* **2012**, *83*, 209 – 215.
[32] J. G. Killian, B. M. Coffey, F. Gao, T. O. Poehler, P. C. Searson, *J. Electrochem. Soc.* **1996**, *143*, 936 – 942.
[33] J. C. Dyre, P. Maass, B. Roling, D. L. Sidebottom, *Rep. Prog. Phys.* **2009**, *72*, 046501.
[34] P. Novák, K. Müller, K. S. V. Santhanam, O. Haas, *Chem. Rev.* **1997**, *97*, 207 – 282.
[35] F. Gschwind, Z. Zao-Karger, M. Fichtner, *J. Mater. Chem. A* **2014**, *2*, 1214 – 1218.
[36] F. Gschwind, J. Bastien, *J. Mater. Chem. A* **2015**, *3*, 5628 – 5634.
[37] F. Gschwind, G. Rodriguez-Garcia, D. J. S. Sandbeck, A. Gross, M. Weil, M. Fichtner, N. Hörmann, *J. Fluorine Chem.* **2016**, *182*, 76 – 90.

Received: September 16, 2016
Published online on November 25, 2016

